DESY 95–151
KEK Preprint 95-93
KEK CP-033
INP MSU Preprint-95-26/390
July 1995

Top Quark Production in the Reaction $e^+e^- \longrightarrow e\nu tb$ at Linear Collider Energies

E. Boos

Deutsches Elektronen-Synchrotron DESY
Institut für Hochenergiephysik IfH, Zeuthen

and

Nuclear Physics Institute, Moscow State University, Russia

Y. Kurihara, Y. Shimizu

KEK, Tsukuba, Japan

M. Sachwitz, H. J. Schreiber

Deutsches Elektronen-Synchrotron DESY
Institut für Hochenergiephysik IfH, Zeuthen

S. Shichanin

Deutsches Elektronen-Synchrotron DESY
Institut für Hochenergiephysik IfH, Zeuthen

and

Institute for High Energy Physics, Protvino, Moscow Region, Russia

ISSN 0418-9833

DESY 95-151
KEK Preprint 95-93
KEK CP-033
INP MSU Preprint-95-26/390

ISSN 0418-9833

July 1995

Top Quark Production in the Reaction $e^+e^- \longrightarrow e\nu tb$ at Linear Collider Energies

E. Boos[1,2], Y. Kurihara[3] M. Sachwitz[1], H. J. Schreiber[1] S. Shichanin[1,4] and Y. Shimizu[3]

[1]DESY-Institut für Hochenergiephysik, Zeuthen, Germany
[2]Nuclear Physics Institute, Moscow State University, 119899, Moscow, Russia
[3]KEK, Tsukuba, Japan
[4]Institute for High Energy Physics, 142284, Protvino, Moscow Region, Russia

Abstract

computed for top masses of 160 to 200 GeV at center-of-mass energies between 0.2 and 2.0 TeV using the packages CompHEP and GRACE. It is demonstrated that $t\bar{t}$-pair production dominates around $\sqrt{s} = 0.5$ TeV, whereas soft photon t-channel exchange contributions grow with increasing energy such that above 1.5 TeV it dominates. Detailed cross section considerations close to the $t\bar{t}$ threshold reveals some peculiar properties. It is shown that a precise top quark mass determination is not significantly hampered by the existence of non-$t\bar{t}$ diagrams. With desirable assumptions on linear collider luminosities the CKM matrix element $|V_{tb}|$ might be measured best at or close to $\sqrt{s} = 2$ TeV.

1 Introduction

After the top quark discovery by the CDF [1] and the D0 [2] collaborations at the Tevatron collider in Fermilab measurements of its properties remain as one of the most important tasks for colliders in the TeV energy range. The values for the top mass of $m_t = 176 \pm 13$ GeV (CDF) and 199 ± 30 GeV (D0) are in a reasonable agreement with 148 to 207 GeV obtained from a combined analysis of the LEP, SLC and neutrino scattering data together with theoretical predictions of the Standard Model (SM) [3] taking into account radiative corrections (see e.g. [4]). The task of top quark coupling measurements is of particular interest due to the coincidence of m_t with the electroweak symmetry breaking scale. Such measurements may give the first indications for deviations from the SM predictions [5].

In previous works it has been demonstrated that future e^+e^- linear colliders provide promising prospects to determine the top quark mass with very high precision (see e.g. [6]) , to probe the top couplings with gauge bosons [7] and the top Yukawa coupling with the Higgs boson [8]. Furthermore, it has been demonstrated that the top quark width respectively $|V_{tb}|$, the Cabibbo-Kobayashi-Maskawa matrix element [9], can be measured by an energy scan in the $t\bar{t}$ threshold region [6], by studying gluon radiation off the top quark or the decay products in $t\bar{t}$ pair production [10], and in single top

$$e^+e^- \to e\,\nu\,t\,b \qquad (1)$$

between its threshold and $\sqrt{s} = 2$ TeV by considering the complete set of Standard Model diagrams. In such a way, all intermediate channels like $e^+e^- \longrightarrow t\,\bar{t}$ with $t \longrightarrow Wb$ and $W \longrightarrow e\nu$, or $e^+e^- \longrightarrow Wtb$ with $W \longrightarrow e\nu$, are taken into account automatically, as well as all interferences between the contributing diagrams[1]. Single top quark production in reaction (1) at LEPII energies has already been studied by our collaboration in ref. [15] using the same procedure.

The paper is organized as follows. In Sect. 2 we discuss the complete tree-level diagrams and describe the calculation method. Results are presented for total cross sections at different energies and top quark masses. Contributions of several subsets of diagrams will also be studied in some detail. Attention is also directed to the cross section behavior close to the $t\,\bar{t}$ pair production threshold. In addition, the physics interest of the reaction $e^-e^- \to e^-\nu\bar{t}\bar{b}$ is discussed. Sect. 3 is devoted to a discussion of the matrix element $|V_{tb}|$. Its measurement prospects are investigated up to very high energies. Sect. 4 contains our summary and conclusion.

2 The cross section of the reaction $e^+e^- \longrightarrow e\nu tb$

In Fig. 1 the complete set of the lowest-order Feynman diagrams contributing to reaction (1) is presented[2].

In order to understand the main properties of reaction (1) better, we have divided these diagrams into three classes. The first class involves the s-channel subprocess $e^+e^- \longrightarrow Wtb$ with the subsequent $W \longrightarrow e\nu$ decay as well as the $t\,\bar{t}$ and W^+W^- pair productions diagrams (with $t \to Wb, W \to e\nu$ and $W \to tb$ decays). The second class contains the photon exchange t-channel diagrams while all remaining diagrams contributing to the $e\nu tb$ final state are collected into the third class. After squaring the diagrams for a given class three cross sections will be obtained, and the remaining interferences between diagrams of different classes are denoted as *interferences* in the following. We are aware that the three classes of diagrams are not gauge invariant. However, it is expected that their main properties are essentially gauge independent.

All results were obtained by means of the two independent computer programs CompHEP[16] and GRACE [17]. CompHEP performs the tree-level symbolic calculations and the generation of optimized FORTRAN codes for

[1]Throughout our paper, reaction (1) involves beside the $e^+\nu_e\bar{t}\bar{b}$ final state also the charge conjugated one $e^-\bar{\nu}_e t\bar{b}$.

[2]Diagrams with a Higgs boson propagator are omitted because of the very small coupling of the Higgs to electrons.

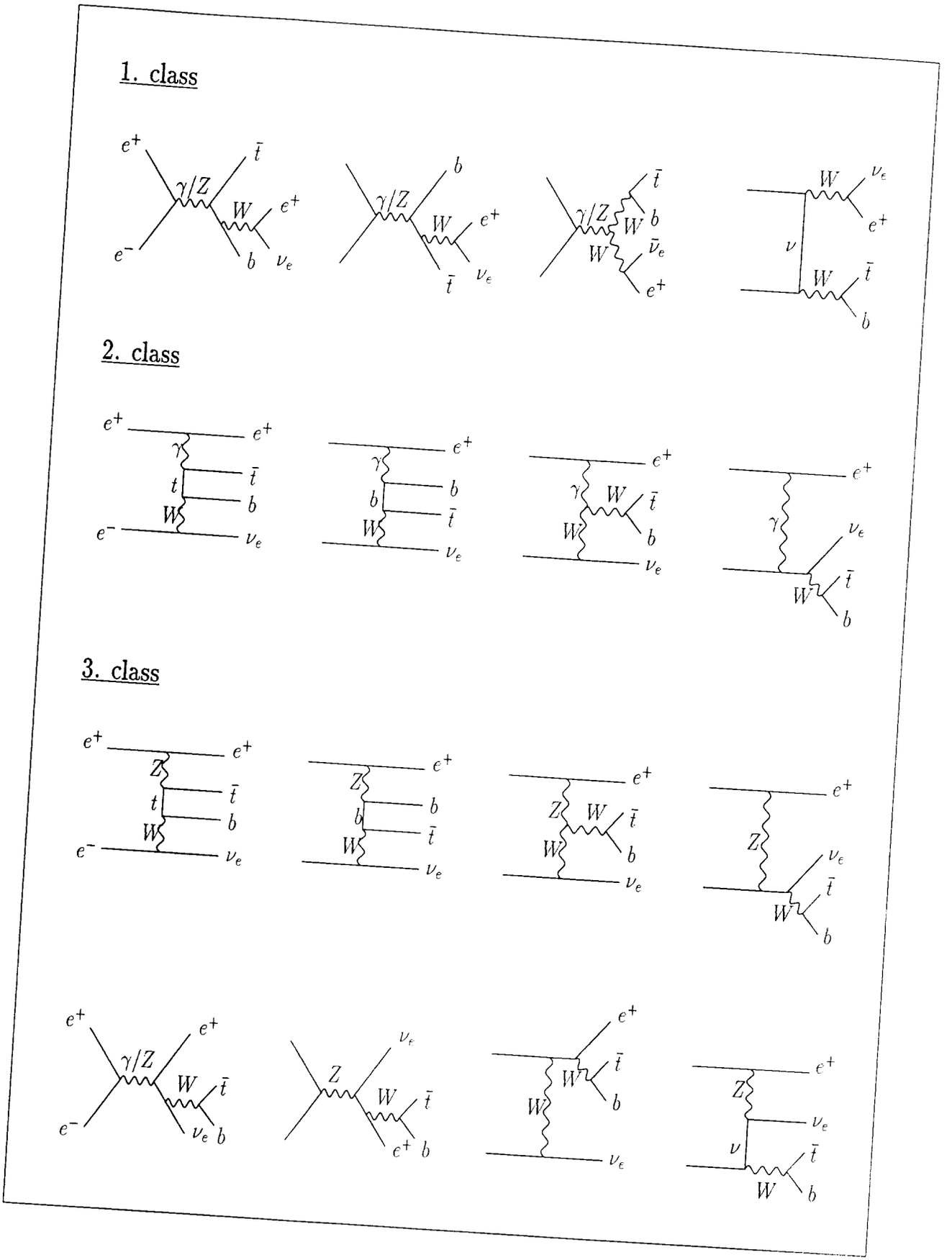

Figure 1: Lowest-order Feynman diagrams for the reaction $e^+e^- \longrightarrow e\nu tb$.

the squared matrix elements, whereas GRACE uses helicity amplitude techniques. We used the adaptive package BASES [18] to integrate over phase space of the 4-body final state.

For all cases considered the agreement between the results of both programs was very good; deviations turned out to be less than 1 %.

The following set of SM parameters has been used in the calculations: m_b = 4.3 GeV, α_{EW} =1/128, $|V_{tb}| = 0.999$, $m_e = 5.11 \cdot 10^{-4}$ GeV, $M_Z = 91.187$ GeV $\sin^2\Theta_W = 0.23$, $M_W = M_Z * \cos\Theta_W$, Γ_Z=2.50 GeV, Γ_W=2.09 GeV, and the tree-level top width for the top masses m_t = 160, 180 and 200 GeV.

All calculations have been done in the t'Hooft Feynman gauge. In order to get confidence in our results several points for the total rate have also been calculated in the unitary gauge. The gauge invariance of our calculations has been confirmed on the level of the numerical integration accuracy of about 0.5 %.

Fig. 2 shows the total cross section for reaction (1), $e^+e^- \longrightarrow e\nu tb$, as function of the cms energy $\sqrt{s}$ between threshold and 2 TeV, for three top mass values.

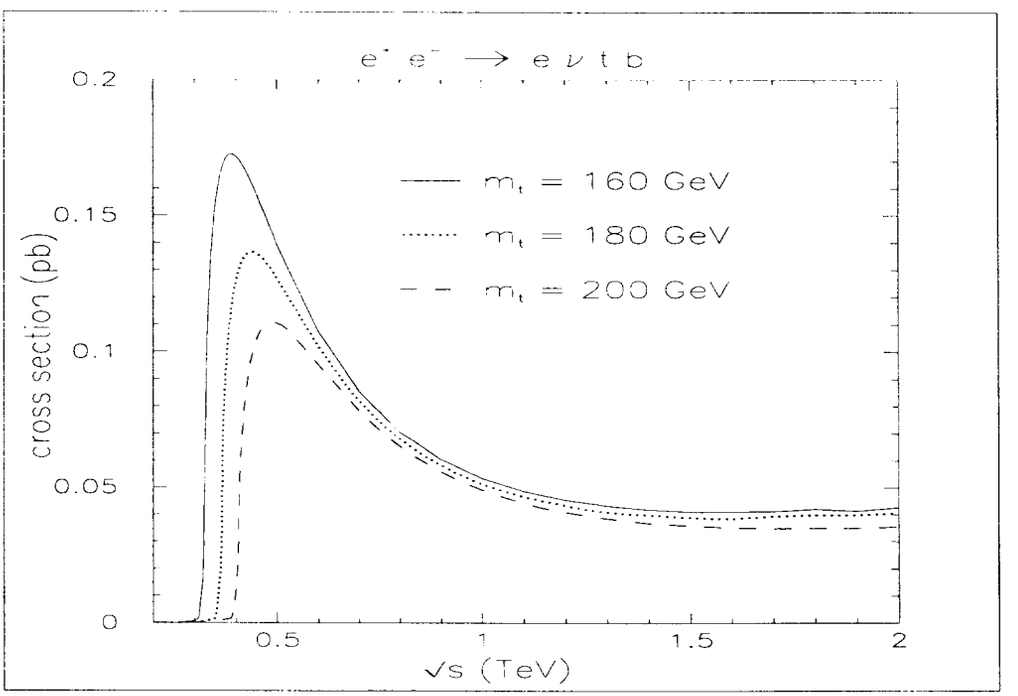

Figure 2: Total cross section for the reaction $e^+e^- \longrightarrow e^+\nu_e\bar{t}b\,(e^-\bar{\nu}_e t\bar{b})$ as function of the cms energy for top quark masses 160, 180 and 200 GeV.

Independent of the top mass, the cross sections have a sharp rise close to the $t\bar{t}$ threshold, a fall-off with $\sim 1/s$ after reaching the maximum and some weak increase with growing energy above $\sim$1.5 TeV. Top mass dependencies

are clearly visible in the energy range below ~0.6 TeV; the cross section at peak value drops by about 20 % when m_t increases from 160 GeV to 200 GeV. At higher energies, top mass dependencies are small.

In Fig. 3 we present the energy dependence of the total rate as well as the contributions of the three classes of diagrams (see Fig. 1), which are denoted as Wtb, *soft photon* and *non-leading* contributions, respectively, and the interferences between them, for $m_t = 180$ GeV. Clearly, the 0.5 TeV energy region is dominated by the 2-to-3 body reaction

$$e^+e^- \longrightarrow Wtb, \qquad (2)$$
$$\hookrightarrow e\nu.$$

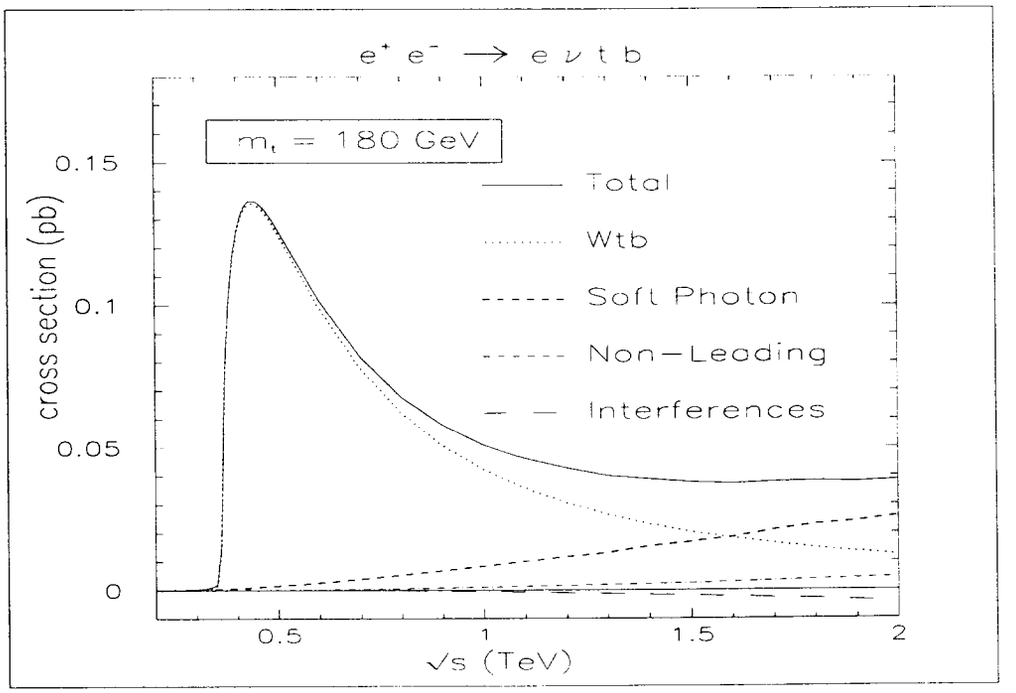

Figure 3: Total cross section for the reaction $e^+e^- \longrightarrow e^+\nu_e\bar{t}b(e^-\bar{\nu}_e t\bar{b})$ as function of the cms energy for $m_t = 180$ GeV (solid line) as well as the contributions of the 'Wtb', the '*soft photon*', '*non-leading*' components and the interferences between them.

Its overwhelming part is associated with $t\bar{t}$ pair production corresponding to the first diagram in Fig. 1. It is also evident that the soft photon contribution (second class of diagrams) becomes more and more important as the energy increases. In particular, it is almost equal to the Wtb rate around 1.5 TeV, whereas at 2 TeV it dominates reaction (1). It is also interesting to point out that the rate for the third class of diagrams, the *non-leading* diagrams, is practically compensated by the negative interference terms between

the diagrams of different classes. Therefore it is justified to neglect these two components in further total cross section estimations.

In addition, the soft photon cross sections have been compared with the cross sections obtained from the improved Weizsäcker-Williams approximation [19]. Acceptable agreement between both calculations has been found; up to 2 TeV differences do not exceed 20 %.

Table 1 collects the cross sections for reaction (1), $e^+e^- \longrightarrow e\nu tb$, at $\sqrt{s} =$ 0.5, 1.0, 1.5 and 2.0 TeV for $m_t = 160$, 180 and 200 GeV. Also the corresponding numbers for the Wtb (with $W \longrightarrow e\nu$) and the soft photon exchange contributions are presented.

$\sqrt{s}$, TeV	m_{top}, GeV	σ_{total}, fb	'Wtb', fb	'*soft photon*', fb
0.5	160	140.0	138.0	1.9
	180	126.6	125.2	1.5
	200	110.4	109.2	1.2
1.0	160	54.0	44.0	10.0
	180	50.0	42.0	8.0
	200	48.6	41.4	7.2
1.5	160	40.8	20.6	20.2
	180	37.2	20.4	16.8
	200	35.0	20.4	14.6
2.0	160	42.8	12.2	30.6
	180	38.2	12.2	26.0
	200	34.8	12.2	22.6

Table 1: Total cross sections for the reaction $e^+e^- \longrightarrow e^+\nu_e\bar{t}b\,(e^-\bar{\nu}_e t\bar{b})$ at four energies and three top quark masses, as well as the rates for the 'Wtb' and '*soft photon*' contributions.

If one is interested in cross sections for other decay modes of the W, e.g. $W \longrightarrow \mu\nu$ or $W \longrightarrow ud$, the rule of thumb is to start from the figures in the 'Wtb' column of Table 1 and multiply them with the ratio of the W branching ratio of

interest to BR($W \longrightarrow e\nu$), since other diagrams which contribute in principle can be neglected. Thus, by summing up all W decay modes one is able to estimate the total top cross section for the reaction $e^+e^- \longrightarrow tb(q\bar{q}', l\nu)$. This is however only reasonable as long as the 'Wtb' contribution is the dominating one, i.e. at $\sqrt{s} \lesssim 0.5$ TeV which corresponds to the energy anticipated for a linear collider in its first stage. At higher energies, in particular at $\sqrt{s} > 1.5$ TeV, the soft photon exchange diagrams have also to be taken into account in order to obtain realistic top quark cross sections in 4-body final states.

In Fig. 4 we present the cross section behavior of reaction (1), $e^+e^- \longrightarrow e\nu tb$, close to the $t\bar{t}$ threshold in more details, again for $m_t = 160$, 180 and 200 GeV.

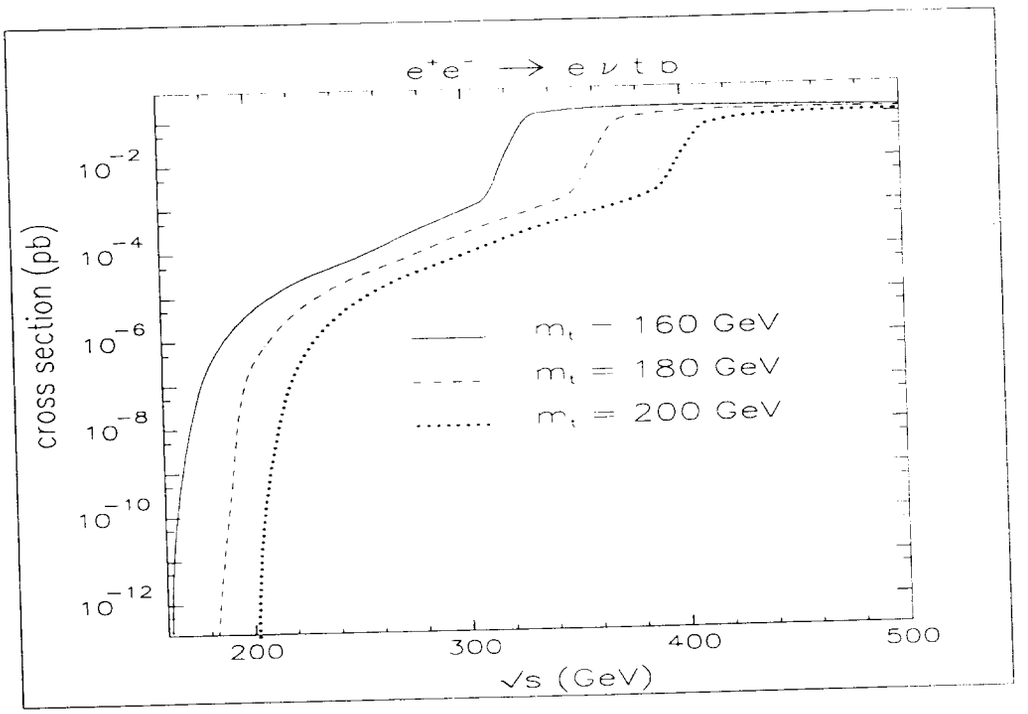

Figure 4: Total cross section for the reaction $e^+e^- \longrightarrow e^+\nu_e\bar{t}b(e^-\bar{\nu}_e t\bar{b})$ as function of the cms energy for top quark masses of 160, 180 and 200 GeV close to the $t\bar{t}$ pair production threshold.

Independent of m_t, a two-step behavior can be noticed. More details about this peculiar behavior can be obtained from Fig. 5, where the total rate has been divided into the three classes of contributions, for $m_t = 180$ GeV.

Clearly, at energies of about 200 GeV only the soft-photon part contributes significantly to reaction (1). Top quark production under such circumstances has been studied in detail in refs. [15, 20] with the conclusion that single top quark production is completely negligible at e.g. LEP II energies. With increasing energy the 'Wtb' contribution rises fast in a way that after crossing the $t\bar{t}$ threshold, it governs the total event rate of reaction (1). The data

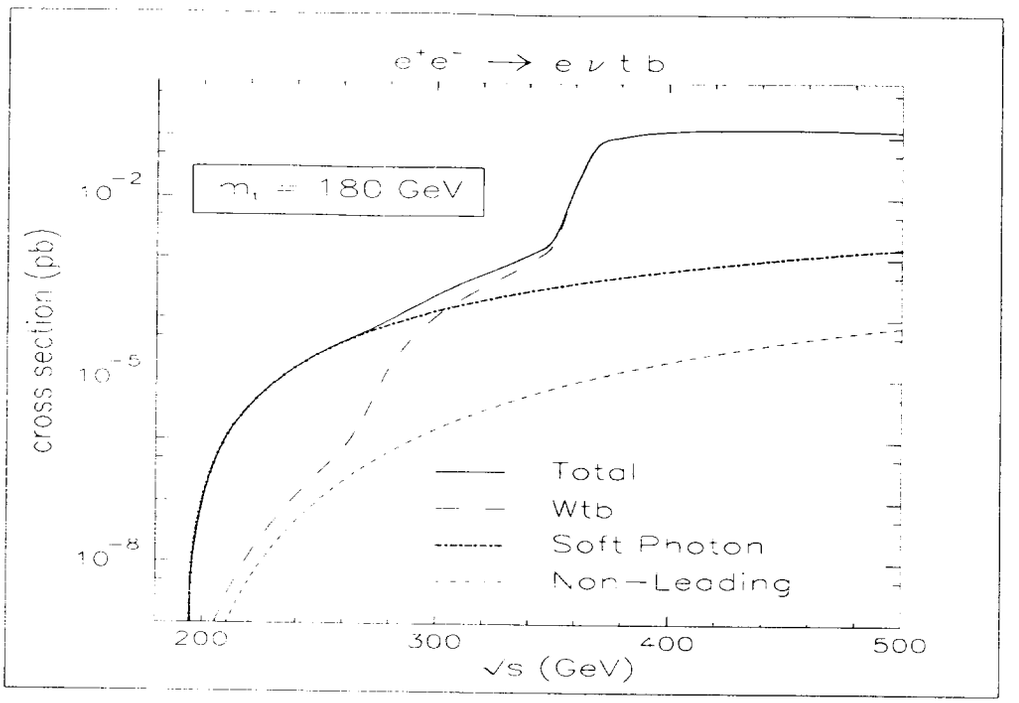

Figure 5: Total cross section for the reaction $e^+e^- \longrightarrow e^+\nu_e\bar{t}b(e^-\bar{\nu}_e t\bar{b})$ as function of the cms energy for $m_t = 180$ GeV (solid line) as well as the contributions of the 'Wtb', the '*soft photon*' and the '*non-leading*' components close to the $t\bar{t}$ pair production threshold.

also indicate the onset of on-shell 'Wtb' production close to $\sqrt{s} = 260$ GeV. The non-leading contribution is the smallest at all energies; it is an order of magnitude below the soft photon component at 500 GeV.

Precise cross section measurements of the reaction $e^+e^- \longrightarrow t\bar{t}$ in the vicinity of its threshold would allow the determination of the top quark mass with an uncertainty of about 300 MeV [21]. Other SM parameters involved in the vertex corrections at $t\bar{t}$ threshold like α_s and Γ_t may also be extracted with good precision. However, all of these studies rely on the assumption that only the first diagram in Fig. 1 corresponding to $t\bar{t}$ pair production supplemented by vertex correction diagrams contributes. All other diagrams which lead to the same topological final state were neglected so far. It will be interesting to see whether they are indeed negligible or affect the top mass measurement significantly. Fig. 6 summarizes our results. The three continuous curves represent the cross sections $\sigma(e^+e^- \longrightarrow t\bar{t})\cdot\mathrm{BR}(t \longrightarrow Wb)\cdot\mathrm{BR}(W \longrightarrow e\nu)$ for three m_t values, 179.7, 180.0 and 180.3 GeV, by taking into account only the $t\bar{t}$-diagram of Fig. 1. As can be seen, the differences between these curves are considerably larger than that caused by the inclusion of all diagrams (dashed curve) with e.g. $m_t = 180$ GeV.

An interesting relation exists between reaction (1), $e^+e^- \longrightarrow e\nu tb$, and the

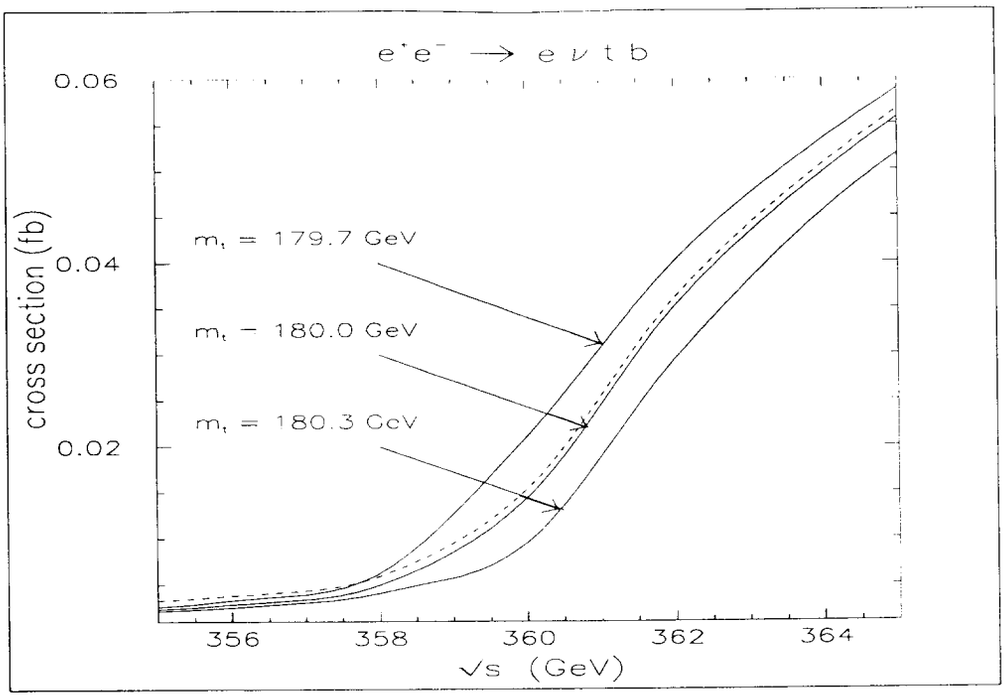

Figure 6: $t\bar{t}$ cross section for the reaction $e^+e^- \longrightarrow e^+\nu_e\bar{t}b(e^-\bar{\nu}_e t\bar{b})$ as function of the cms energy for top quark masses 179.7, 180.0 and 180.3 GeV. The dashed curve corresponds to the cross section for $m_t = 180$ GeV including all diagrams of Fig. 1.

process

$$e^-e^- \longrightarrow e^-\nu\bar{t}b. \tag{3}$$

In the latter case, all s-channel diagrams of Fig. 1 are absent, and the remaining t-channel diagrams have to be doubled for cross section estimations due to the existence of two identical electrons in the initial state. This doubling is equivalent to the summation of the $e^+\nu_e\bar{t}b$ and its charge conjugate final state $e^-\nu_e t\bar{b}$ in the e^+e^- case. Additional interference terms caused by doubling the diagrams are very small, so that the cross sections for reaction (3) are to a very good approximation equal to those of reaction (1), including its charge conjugated state. Therefore, e^-e^- collision provides in particular at large energies a very clean environment for soft photon exchange studies, and their cross sections can be obtained from Fig. 2 respectively Table 1. It might be that due to lesser background precise determinations of SM parameters can be carried out better in e^-e^- than in e^+e^- collisions especially at $\sqrt{s} \gtrsim 1.5$ TeV. An example is presented in the next section.

3 Wtb coupling and the measurement of the $|V_{tb}|$ matrix element

In the SM the coupling of the top quark to the W boson and the b-quark has V-A structure and is proportional to the square of the CKM matrix element $|V_{tb}|$

$$\Gamma_{\mu}^{tWb} = \frac{e}{2\sqrt{2}\sin\Theta_W}|V_{tb}|^2\gamma_{\mu}(1-\gamma_5). \tag{4}$$

Measurements of $|V_{tb}|$ and/or Γ_t are known to be nontrivial due to the very short lifetime of the heavy top quark. In the past several methods have been proposed to measure $|V_{tb}|$ and Γ_t. They rely either on an energy scan and the top quark momentum respectively forward-backward asymmetry measurements in the $t\bar{t}$ threshold region [6, 21], or the study of soft gluon or photon radiation pattern in $t\bar{t}$ events above the $t\bar{t}$ threshold energy [10, 22], or event rate measurements of the process $e^+e^- \longrightarrow tW^-\bar{b}$ after removing $t\bar{t}$ events, again well above the $t\bar{t}$ threshold [12]. The accuracy of $|V_{tb}|$, however, depends significantly on SM parameters, the beam energy spectrum, higher order α_s corrections and statistics. In general, the precision estimated for $|V_{tb}|$, $\delta|V_{tb}|$, turns out to be of ~ 20 % at best.

In this section we investigate the sensitivity which can be achieved for $|V_{tb}|$ when reaction (1), $e^+e^- \longrightarrow e\nu tb$, at cms energies between 0.5 TeV and 2 TeV is considered. As stated in Sect. 2, at $\sqrt{s} = 0.5$ TeV reaction (1) is practically completely dominated by $t\bar{t}$ production, whereas at $\sqrt{s} = 2$ TeV soft photon exchange diagrams (second class in Fig. 1) contribute mostly. In $t\bar{t}$ pair production, with subsequent decay of the top quark, information of its coupling from event rates is practically lost because the $|V_{tb}|$ dependence of the tWb vertex is basically canceled by the t-quark Breit-Wigner propagator dependence. Thus, the measurement of $|V_{tb}|$ at $\sqrt{s} = 0.5$ TeV with best sensitivity requires a cut on the Wb respectively $e\nu b$ invariant mass in reaction (1) in order to remove $t\bar{t}$ pair production or to enhance single top quark production (see also ref. [12]). The size of the cut is in principle unknown and influences the event rate which in turn determines the sensitivity on $|V_{tb}|$, $\delta|V_{tb}|$. The quantity which we calculate represents the 'single' top quark production cross section

$$\sigma_{\Delta}(V_{tb}) = \int_{M_{min}}^{M_t-\Delta} dM \frac{d\sigma^{tot}}{dM} + \int_{M_t+\Delta}^{M_{max}} dM \frac{d\sigma^{tot}}{dM}, \tag{5}$$

where $M \equiv M_{Wb}(= M_{e\nu b})$ is the invariant mass of the $(e\nu b)$ system, $M_{min} =$

$M_t + M_b$, $M_{max} = \sqrt{s}$ - $M_t - M_b$, and Δ, the cut value, which has been chosen to vary between zero and 10 GeV. The cross section (5) has been calculated for several $|V_{tb}|$ values between 0.7 and 1.2 (in steps of 0.05) and converted into event rates by taking into account the luminosities $\mathcal{L}$ as given in Table 2 integrated over 10^7 sec, a typical year of running.

$\sqrt{s}$, TeV	Luminosity $\mathcal{L}$, $cm^{-2}sec^{-1}$
0.5	$5 \cdot 10^{33}$
1.0	$2 \cdot 10^{34}$
1.5	$3 \cdot 10^{34}$
2.0	$5 \cdot 10^{34}$

Table 2: Desirable luminosities for a possible e^+e^- linear collider as proposed in ref. [23].

The errors on $|V_{tb}|$ expected for three-standard deviations with respect to the SM expectations (with $|V_{tb}| = 0.999$) are plotted in Fig. 7 against Δ at $\sqrt{s}$= 0.5, 1.0, 1.5 and 2.0 TeV, for m_t= 180 GeV. An event selection efficiency ϵ of 100 % has been assumed. As can be seen, the higher the energy $\sqrt{s}$, the better is the accuracy on $|V_{tb}|$. Thus, very promising measurements of $|V_{tb}|$ will be possible at $\sqrt{s} = 2$ TeV even if one takes into account event selection efficiencies ϵ less than unity and somewhat lower luminosities[3].

Further, at $\sqrt{s} = 0.5$ TeV a dramatic cut variation of the $\delta|V_{tb}|$ occurs, which indicates that for Δ close to 1-2 GeV an optimized situation exists. It is also clearly visible that the expectation for the case of no $M(e\nu b)$-cut (i.e. $\Delta = 0$) the $|V_{tb}|$ sensitivity drops sharply because of the insensitivity of the overwhelming $t\bar{t}$ events to $|V_{tb}|$. Our $\delta|V_{tb}|$ value of $\sim$0.055 for $\Delta = 5$ GeV at $\sqrt{s} = 0.5$ TeV is consistent with the analogous findings of ref. [12] taking into account the different luminosities assumed, the different W decay modes and $\epsilon \simeq$30 %. However, it is worth emphasizing that the accuracy of $|V_{tb}|$ can be significantly improved at $\sqrt{s} = 2$ TeV provided the linear collider is able to deliver a luminosity close to $5 \cdot 10^{34}$ cm^{-2} sec^{-1}. Such $|V_{tb}|$ measurements do not suffer from theoretical uncertainties due to higher order QCD corrections and do not require an optimized Δ-cut (see Fig. 7). Remaining $t\bar{t}$ events might be easily removed by a soft cut of about 5 GeV which is more in accord with experimental resolutions of hadronic calorimeters, than a value of 1-2 GeV preferred at $\sqrt{s} = 0.5$ TeV.

[3]The sensitivity on $|V_{tb}|$ worsens with $1/\sqrt{\epsilon}$ and $1/\sqrt{N}$, where N is the number of events expected.

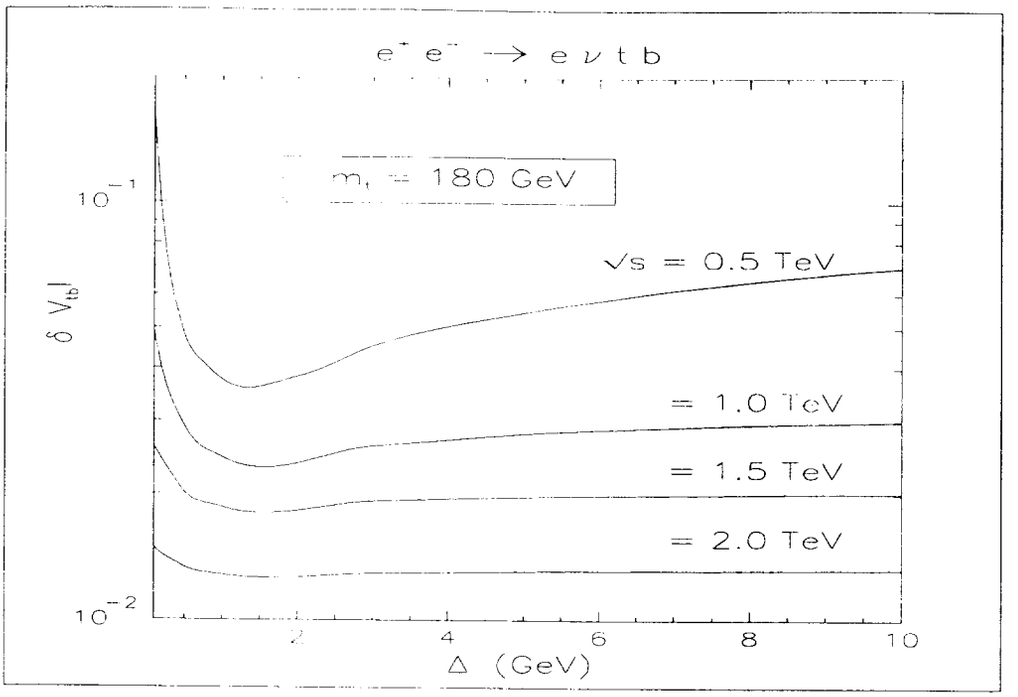

Figure 7: Sensitivity of $|V_{tb}|$ expected for three-standard deviations with respect to the SM predictions against the cutting parameter Δ for several energies.

4 Summary and conclusion

Reaction (1), $e^+e^- \longrightarrow e\nu tb$, has been studied in the energy range 0.5 to 2 TeV and for top quark masses of 160, 180 and 200 GeV. The results were obtained by means of two independent computer programs, CompHEP and GRACE, and the adaptive Monte Carlo package BASES has been used for phase space integration. Both approaches yield cross section values in very good agreement with each other, and gauge invariance has been confirmed on the level of the numerical integration accuracy.

The cross section for reaction (1) rises very sharply after threshold, reaches a maximum somewhat above $\sqrt{s} = 2m_t$ and decreases like $\sim 1/s$ with increasing energy. At very large $\sqrt{s}$, however, the total cross section rises slowly due to a permanently growing importance of the soft photon t-channel exchange contributions (corresponding to the second class of diagrams in Fig. 1). Other non-$t\bar{t}$ contributions to the process $e^+e^- \longrightarrow e\nu tb$ were found to be very small and are largely canceled by the negative interferences between diagrams of the different classes as shown in Fig. 1. In particular, at $\sqrt{s} = 0.5$ TeV, the possible energy of an e^+e^- linear collider in its first phase, practically all events are due to $t\bar{t}$ pair production, while at 2 TeV about 2/3 of the events in reaction (1) are produced by soft photon t-channel exchange. It is

further demonstrated that below $t\bar{t}$ threshold soft photon contributions also dominate the total event rate. However, the number of events expected is so small that physics studies are strongly restricted even if one assumes very large luminosities. We have also shown that top quark mass measurements by an energy scan in the $t\bar{t}$ threshold region are not significantly hampered by the effects of all diagrams that contribute in addition to the $t\bar{t}$ diagram.

Under reasonable assumptions for the luminosity of an e^+e^- linear collider we have studied the accuracy with which the CKM matrix element $|V_{tb}|$ can be studied. At $\sqrt{s} = 0.5$ TeV, the removal of the dominating $t\bar{t}$ events which are insensitive to $|V_{tb}|$ limits the accuracy. The best cut for $t\bar{t}$ event rejection in the Wb respectively $e\nu b$ invariant mass has a value of 1 - 2 GeV which is significantly below the anticipated resolution of hadronic calorimeters. The best sensitivity for $|V_{tb}|$ might be obtained at $\sqrt{s} = 2$ TeV where single top soft photon production dominates. It is also worthwhile to note that no M($e\nu b$)-cut value optimization is required at such large energies and that $|V_{tb}|$ measurements do not suffer from theoretical uncertainties due to higher order QCD corrections as expected in the $t\bar{t}$ threshold region. In this context a high energy e^-e^- collider offers an advantage because the event rate expected for $e^-e^- \longrightarrow e^-\nu\bar{t}b$ is practically the same as that for reaction (1) with the absence of s-channel background.

Acknowledgments

We would like to thank V. Ilyin and A. Pukhov for discussions and the help with CompHEP calculations. E.B. and S. Sh. are grateful to P. Söding for his interest and support, and to DESY-IfH Zeuthen for the kind hospitality. The work has partially been supported by the ISF grant No. M9B000 and No. M9B300, by the INTAS grant INTAS-93-1180 and by the Russian Foundation for Fundamental Researches RFFR-95-02-03704.

References

[1] F. Abe et al., Phys. Rev. Lett. **74** (1995) 2626.

[2] S. Abachi et al., Phys. Rev. Lett. **74** (1995) 2632.

[3] S. L. Glashow, Nucl. Phys. **22** (1961) 579;
S. Weinberg, Phys. Rev. Lett. **19** (1967) 1264;
A. Salam, Elementary Particle Theory, ed. by N. Svartholm, Stockholm (1968) 367.

[4] The LEP Collaborations and the LEP Electroweak Working Group, CERN/PPE/94-187, from presentations at the 27th International Conference on High Energy Physics, Glasgow (1994).

[5] R.D. Peccei, S. Peris and X. Zhang, Nucl. Phys. **B349** (1991) 305.

[6] K. Fujii, T. Matsui and Y. Sumino, Phys. Rev. **D50** (1994) 4341.

[7] M.E. Peskin, Workshop on Physics and Experiments with linear Colliders, Saariselkä, Finland, 1991, p.1;
D.O. Carlson, E. Malkawi and C.-P. Yuan, Phys. Lett. **B337** (1994) 145;
T.Rizzo, Phys. Rev. **D50** (1994) 4478.

[8] A.Djouadi, J.Kalinovski and P.Zerwas Z. Phys. **C54** (1992) 255;
E.Boos et al. , Z. Phys. **C56** (1992) 487.

[9] M. Kobayashi and T. Maskawa, Prog. Theor. Phys. **49** (1973) 652.

[10] V.A. Khose, L.H. Orr and W.J. Stirling, Nucl. Phys. **B378** (1992) 413;
V.A.Khose, J.Ohnemus and W.J.Stirling Phys. Rev. **D49** (1994) 1237.

[11] S. Ambrosanio and B. Mele, Z. Phys. **C63** (1994) 63.

[12] N.V. Dokholian and G.V. Jikia, Phys. Lett. **B336** (1994) 251.

[13] S. Dawson, Nucl. Phys. **B249** (1985) 42;
S. Willenbrock and D.A. Dicus, Phys. Rev. **D34** (1986) 155;
S. Dawson and S. Willenbrock, Nucl. Phys. **B284** (1987) 449;
C.-P. Yuan, Phys. Rev. **D41** (1990) 42;
T. Moers, R. Priem, D. Rein and H. Reitler, Proc. of the Large Hadron Collider Workshop, Aachen, 418 (1990);
R.K. Ellis and S. Parke, Phys. Rev. **D46** (1992) 3785;
G.V. Jikia and S.R. Slabospitsky, Phys. Lett. **B295** (1992) 136;
D.O. Carlson and C.-P. Yuan, Phys. Lett. **B306** (1993) 386;
E. Malkawi and C.-P. Yuan, Phys. Rev. **D50** (1994) 4462.

[14] A.S. Belyaev, E.E. Boos and A.P. Heinson, preprint in preparation.

[15] E. Boos et al., Phys. Lett. **B326** (1994) 190.

[16] E.E. Boos et al., in the Proceedings of the XXVIth Rencontre de Moriond, ed. by J. Tran Than Van, Edition Frontiers, p.501 (1991);
E.E. Boos et al., in the Proceedings of the Second International Workshop on Software Engineering, ed. by D. Perret-Gallix, World Scientific, p.665 (1992);
V.A. Ilyin, D.N. Kovalenko and A.E. Pukhov, INP MSU Preprint-95-2/366, Moscow State University, (1995).

[17] T. Ishikawa et al., GRACE manual, KEK report 92-19, 1992.

[18] S. Kawabata, Comp. Phys. Commun. 41 (1986) 127.

[19] S. Frixione, M. Mangano, P. Nason and G. Ridolfi, Phys. Lett. **B314** (1993) 339;
R.P. Kauffman, Phys. Rev. **D41** (1990) 3343;
V.M. Budnev, I.F. Ginzburg, G.V. Meledin and V.G. Serbo, Phys. Rep. **15C** (1975) 1.

[20] O. Panella, G. Pancheri and Y.N. Srivastara, Phys. Lett. B318 (1993) 214;
K. Hagiwara, M. Tanaka and T. Stelzer, Phys. Lett. **B325** (1994) 521;

[21] K. Fujii, KEK preprint 92-153 (1992);
P. Igo-Kemenes, Workshop on Physics and Experiments with Linear Colliders, Waikoloa, Hawaii, 1993, p.95.

[22] G.V. Jikia, Phys. Lett. **B257** (1991) 196;
G.F. Abu Leil, preprint DTP/92/84, 1992.

[23] B.H. Wiik, talk given at the TESLA meeting, Frascati, Nov. 1994.